

## REVIEW

# Introduction to bioimaging-based spatial multi-omic novel methods

Yan Yan<sup>1,2,†</sup>, Liheng Yang<sup>3,†</sup>, Leyuan Meng<sup>4,†</sup>, Haochen Su<sup>5</sup>, Cheng Zhou<sup>6</sup>, Le Yu<sup>7</sup>, Zhengtu Li<sup>8</sup>, Xu Zhang<sup>9,10,\*</sup>, Huihua Cai<sup>11,\*</sup>, Juntao Gao<sup>1,2,10,12,13,\*</sup>

<sup>1</sup> MOE Key Laboratory of Bioinformatics, Tsinghua University, Beijing 100084, China

<sup>2</sup> Center for Synthetic & Systems Biology, Tsinghua University, Beijing 100084, China

<sup>3</sup> Seaver College, Pepperdine University, Malibu, CA 90263, USA

<sup>4</sup> College of Animal Sciences, Heping campus, Jilin University, Jilin 130062, China

<sup>5</sup> Sidney Sussex College, Sidney Street, Cambridge CB2 3HU, United Kingdom

<sup>6</sup> Department of Radiation Oncology, Nanfang Hospital, Southern Medical University, Guangzhou 510515, China

<sup>7</sup> Foshan Protogene Tech. Co. Ltd, Foshan 510168, China

<sup>8</sup> State Key Laboratory of Respiratory Disease, National Clinical Research Center for Respiratory Disease, Guangzhou Institute of Respiratory Health, the First Affiliated Hospital of Guangzhou Medical University, Guangzhou 510120, China

<sup>9</sup> Beijing Institute of Collaborative Innovation, Beijing 100094, China

<sup>10</sup> Department of Automation, Tsinghua University, Beijing 100084, China

<sup>11</sup> Department of Obstetrics and Gynecology, Guangdong Provincial People's Hospital, Guangdong Academy of Medical Sciences, Guangzhou 511436, China

<sup>12</sup> Bioinformatics Division, BNRist, Tsinghua University, Beijing 100084, China

<sup>13</sup> Institute for TCM-X, Tsinghua University, Beijing 100084, China

\* Correspondence: [caihuihua@gdph.org.cn](mailto:caihuihua@gdph.org.cn); [zhangx@jingjinji.cn](mailto:zhangx@jingjinji.cn); [jtgao@tsinghua.edu.cn](mailto:jtgao@tsinghua.edu.cn)

Received November 7, 2022; Revised January 26, 2023; Accepted March 13, 2023

**Background:** Spatial multi-omics are demonstrated to be a powerful method to assist researchers on genetic studies. In this review, bioimaging-based spatial multi-omics techniques such as seqFISH+, merFISH, integrated DNA seqFISH+, DNA merFISH, and MINA are introduced along with each technique's probe design, development, and imaging processes.

**Results:** seqFISH employed 4–5 fluorophores to barcode and conducted multiple rounds of hybridization, in order that mRNA can be identified through color-coding. seqFISH+ added 60 pseudo-color and distributed them equally into three channels to enhance imaging power, in order that *i.e.*, 24,000 genes can be imaged in total. merFISH utilized 4 out of 16 Hamming distance to innovatively provide a robust error-detecting method. MINA, a methodology combining merFISH (multiplexed error-robust fluorescence *in situ* hybridization) and chromosomal tracing, enabled multiplexed genomic architecture imaged in mammalian single cells. Optical reconstruction of chromatin architecture (ORCA) a method that could conduct DNA path tracing in nanoscale manner with kilobase resolution, an FISH variation that improved genetic resolution, enable high-precision fiducial registration and sequential imaging, and utilized Oligopaint probe to hybridize the short genomic region ranging from 2 to 10 kilobase. ORCA then prescribes these short section primary probes with individual barcodes to attach fluorophore and to be imaged.

**Conclusion:** This review concentrated on providing a comprehensive overview for these spatial-multi-omics techniques with the intention on helping researchers on selecting appropriate technique for their research.

**Keywords:** FISH; multiplex FISH; super-resolution imaging; gene regulation

<sup>†</sup> These authors contributed equally to this review.

**Author summary:** In this review, we introduced five different multiplex FISH methods used for image-based spatial multi-omics: seqFISH+, merFISH, DNA seqFISH+, DNA merFISH, and MINA. We provided a systematic collective perspective to review these FISH methods that could significantly benefit researchers on conducting their studies in the field. Our study provided an informative survey on these multiplex FISH methods. Therefore, this review would provide better understanding for researchers in the community to help them select the proper method, in order to understand the molecular mechanism in life sciences.

## INTRODUCTION

DNA fluorescence *in situ* hybridization (FISH) enables mapping of spatial position of genomic organizations of single cells and is used to detect or verify the spatial interaction between the basic regulatory units of genome 3D structure, such as enhancer and promoter [1]. As a ligation-free method, FISH provides geometric, but not topological, information of 3D genomes. Recent sequential FISH techniques enables mapping of mammalian cell chromatin organizations [2].

In the exciting new era of spatial multi-omics, at least two novel requirements need to be met. The first one, of course, is to image genomic loci at large-scale, such as thousands of genes, at the same time. The second one, is to image every single genomic locus with much higher resolution, than the traditional one, in order to resolve the optical overcrowding of mRNA or genomic loci. Two questions need to be addressed to meet this requirement. One is microscopy which should provide much higher resolution than traditional diffraction-limit microscope. Optical resolution has always been challenging for the universal profiling of mRNA transcripts in single cells. Each mRNA demonstrates a specific diffraction-limit position during imaging; therefore, tens of thousands of mRNAs generated an optical crowding which hindered mRNAs from being resolved and prevented the implementation of high throughput spatial profiling procedures [3,4]. Fortunately, various super-resolution microscopy was developed during the last two decades [5–8]. For example, three important and novel developed high-throughput FISH techniques (SABER-FISH [9], FRET-FISH [10], CRISPR-FISHer [11]) are briefly discussed as follows. SABER-FISH [9] allows for the identification and quantification of specific RNA molecules within cells or tissues. It is similar to conventional FISH, which uses fluorescent probes to bind to specific RNA sequences. SABER-FISH, however, employs a bead-based approach, where the probes are attached to beads and then hybridized to the target RNA in the sample. After hybridization, the beads are imaged and the fluorescence signal is used to identify and quantify the target RNA. This technology enables high-throughput and multiplexed quantification of multiple RNAs in the same sample. FRET-FISH [10] (Förster Resonance Energy Transfer *in situ*

hybridization) utilized the non-radiative energy transfer process that occurs between fluorescent donor and acceptor molecules to detect and quantify specific RNA molecules in cells and tissues. Researchers could quantify and detect the target RNA in the specimen by measuring acceptor fluorescence. FRET-FISH functioned as a powerful FISH method for multiplexed and highly sensitive *in situ* RNA specification. CRISPR-FISHer [11] used CRISPR-Cas system to introduce fluorescent probes to targeted sequences in the genome, and CRISPR-FISHer used FISH to detect and visualize these hybridized probes. In addition, an interesting novel FISH method, pai-FISH was developed very recently, which utilized three rounds of probing and bond sequences to amplify the corresponding signals. In this method,  $\pi$ -shape target probe was hybridized to the targeted region at first. The  $\pi$ -shape target probe consisted of two complimentary (8 nt bond) parabola shaped probes. The top region of the two complementary parabola shaped probes constitutes a U-shaped (secondary) probe to make fluorescent hybridizations stable. Thereafter U-shape (secondary) probe was attached to  $\pi$ -shape target probe. A bigger U-shaped amplified (tertiary) probe was attached to U-shape (secondary) probe to intensity fluorescent signals by accepting multiple signal probes using U-shaped amplified (tertiary) probes. Pai-FISH enabled more hybridizations for each target region through multiple rounds of probing and bond sequences. When compared with conventional smFISH (single molecule fluorescence *in situ* hybridization), pai-FISH demonstrated intensified fluorescent signaling under the same detection capacity.

The second one, is FISH probes, which should be able to label every single genomic locus with kilo-base resolution. There are several reasons for this issue: (1) The length of a typical enhancer, which is one of the key regulatory elements, can be on average only ~500 base pairs (bp) long, ranging from as little as 100 bp [12–14] to several kilobases (kb) [15,16]. (2) The average length of a single human gene is around 50 kb with significant deviation [17]. (3) The genomic length of a typical TAD (topological associated domain) or contact domain, which provides spatial space for chromatin interactions and for regulatory elements to work, is around 0.2–1 megabases (Mb).

To fulfill these requirements, several multiplex FISH

methods were developed during the last several years for spatial multi-omics, including seqFISH [18], seqFISH+ [19], merFISH (multiplexed error-robust fluorescence

*in situ* hybridization) [20,21], DNA seqFISH+, DNA merFISH, and MINA [22] (Fig. 1 and Table 1), etc. They are introduced below.

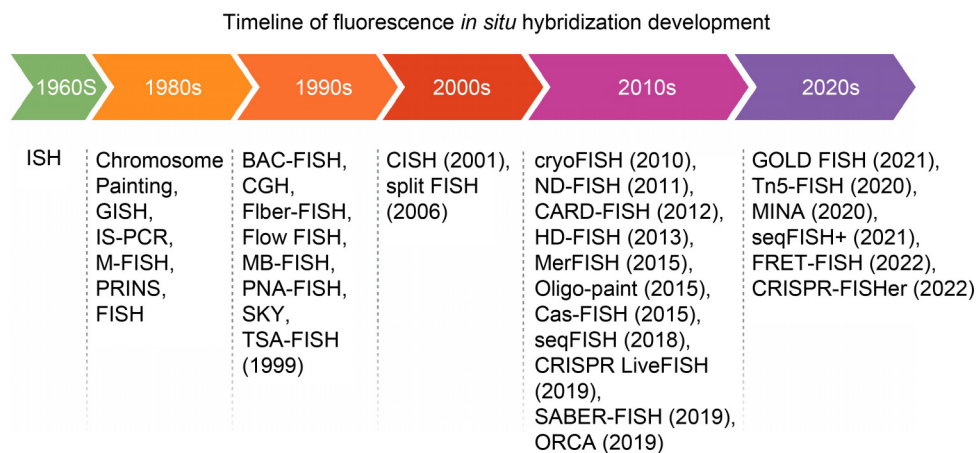


**Figure 1.** A timeline of FISH method is demonstrated chronologically, *in situ* hybridization was initially developed in the 1960s.

**Table 1** The spatial resolution, time cost, multiplexed (multiplexed or non-multiplexed), throughput (high-throughput or non-high-throughput), automatization, and references are listed in this table

		Spatial resolution (confocal post 2000 s/ spatial resolution)	Time cost	Complexity (multiplexed/ non-multiplexed)	Throughput (high-throughput/ non-high-throughput)	Automatization (yes/no)	Refs.
2020s	Tn5-FISH	Confocal	~ 1 day	Non-multiplexed	Non-high-throughput	No	[23]
	M-DNA-FISH	Super resolution	–	Multiplexed	High-throughput	Yes	[24]
	MINA	Super resolution	~ 7 days	Multiplexed	High-throughput	Yes	[25]
	seqFISH+	Confocal	~ 60 hours (depending on the amonut of gene)	Multiplexed	High-throughput	Yes	[26]
	FRET-FISH	Confocal	~ 2 weeks	Multiplexed	High-throughput	Yes	[10]
	CRISPR-FISHer	Confocal	~ 60 hours/2 days	Multiplexed	High-throughput	Yes	[11]
	MB-FISH	–	–	–	–	Yes	[27]
2010s	cryoFISH	Confocal	–	Non-multiplexed	Non-high-throughput	No	[28]
	HD-FISH	Confocal	~ 1 week	Non-multiplexed	Non-high-throughput	No	[29]
	merFISH	Super resolution	~ 1 day	Multiplexed	High-throughput	Yes	[2, 20]
	Oligopaint	Super resolution	~ 4 days	Non-multiplexed	Non-high-throughput	No	[30, 31]
	Cas-FISH	Confocal	~ 1 week	Non-multiplexed	Non-high-throughput	No	[32]
	seqFISH	Super resolution	~ 2 days	Non-multiplexed	Non-high-throughput	No	[18]
	CRISPR LiveFISH	Confocal	–	Multiplexed	High-throughput	Yes	[33]
	SABER-FISH	Confocal	–	Multiplexed	High-throughput	Yes	[9]
ORCA	Super resolution	–	Multiplexed	High-throughput	Yes	[34]	
2000s	CISH	Confocal	~ 2 weeks	Non-multiplexed	Non-high-throughput	No	[35]
	ND-FISH	Confocal	~ 1 week	Non-multiplexed	Non-high-throughput	No	[36]
	CARD-FISH	Confocal	~ 2 days	Non-multiplexed	Non-high-throughput	No	[37]
	split FISH	Confocal	–	Non-multiplexed	Non-high-throughput	No	[38]
1990s	BAC-FISH	Confocal/widefield	~ 2 days	Non-multiplexed	Non-high-throughput	No	[39]
	CGH	Confocal/widefield	–	Non-multiplexed	Non-high-throughput	No	[40]
	Fiber-FISH	Confocal/widefield	–	Non-multiplexed	Non-high-throughput	No	[41]

*(continued)*

	Spatial resolution (confocal post 2000 s/ spatial resolution)	Time cost	Complexity (multiplexed/ non-multiplexed)	Throughput (high-throughput/ non-high-throughput)	Automatization (yes/no)	Refs.	
1990s	Flow FISH	Confocal/widefield	–	Non-multiplexed	Non-high-throughput	No	[42]
	PNA-FISH	Confocal/widefield	–	Non-multiplexed	Non-high-throughput	No	[43]
	SKY (spectral karyotyping)	Confocal/widefield	–	–	–	Yes	–
	TSA-FISH	Confocal/widefield	–	–	–	–	–
1980s	Chromosome painting	–	–	–	–	–	–
	GISH (genomic <i>in situ</i> hybridization)	–	~ 1 day	Non-multiplexed	Non-high-throughput	No	–
	IS-PCR	–	–	–	–	–	–
	M-FISH (multicolor FISH)	–	–	–	–	Yes	–
	PRINS (Primed in sity labeling)	–	~ 2 hours	Non-multiplexed	Non-high-throughput	No	[44]
	FISH	–	~ 1 day	Non-multiplexed	Non-high-throughput	No	[45, 46]
1960s	ISH	–	~ 1 hour	Non-multiplexed	Non-high-throughput	No	[47, 48]

“–” marks information that were not listed in the publication, and therefore not listed in the table above.

## seqFISH+

SeqFISH+ can label more than 10,000 genes in a single cell. To label more mRNA, it is most important to overcome limited optical density. SeqFISH previously used the expansion microscopy method to overcome the issue of light density, allowing the technique to detect thousands of transcripts per cell.

SeqFISH+ uses a multi-round hybridization approach. After completing every round of hybridization, the signal from the previous round was washed off, and a different pseudo-color was used for imaging in the next round of hybridization to distinguish the pseudo-color from the previous round.

In this method, for every round, a total of three fluorescent channels were used, with each channel completing 20 rounds of hybridization, that is, 20 pseudocolors used in each channel. In each round of hybridization, for the four readouts in every target gene, three readouts were used for the coding of target gene, while the fourth readout was used for the correction of the completed barcoded gene. As a result, a total of  $3 \times 20^3 = 24,000$  genes can be labeled and imaged.

## Development of seqFISH+

In seqFISH+ [19], mRNA of 10,000 genes from cleared NIH/3T3 fibroblast cells were randomly selected to demonstrate transcriptome-level profiling, and the localization of individual transcript was specified/identified. Building on top of seqFISH [18], seqFISH+ expanded the color palettes from four or five

colors used in seqFISH to 60 “pseudocolors (Fig. 2A)”. By using 60 pseudocolors, seqFISH+ could efficiently image each mRNA dot under different diffraction limit through diluting the mRNA molecules into 60 individual images. Then, three fluorescent channels were employed in seqFISH+ to each barcode, with  $20^3$  (*i.e.*, 8,000) genes leading to a total of 24,000 genes being imaged. Imaging time for seqFISH+ was reduced to one eighth of seqFISH since the adoption of 60 pseudocolors. Compared to seqFISH, fewer genes (16,384) could be barcoded using only four colors, and longer time would be needed as well.

## Probe design

The primary component of seqFISH+ probe is the readout and target region, and the target region obtained its sequence from each gene’s CDS (coding sequence) region or UTRs (untranslated region). Every target region has a length of 2 nt, which is 2 nt less than merFISH target region. When selecting marker genes, designer should avoid housekeeping genes, histone, and very expressed genes. The readout sequence of seqFISH+ is 15 nt.

After adding T7 sequences to target sequence along with readout sequence and amplification primer through PCR, a completed seqFISH+ probe demonstrated to be 93 nt in total length. T7 sequences were added to the end of the probe through PCR. 1 M NaOH was used to denature excessive RNA, 1 M acetic acid was used for neutralization, and probes are ready to deploy after ethanol precipitation.

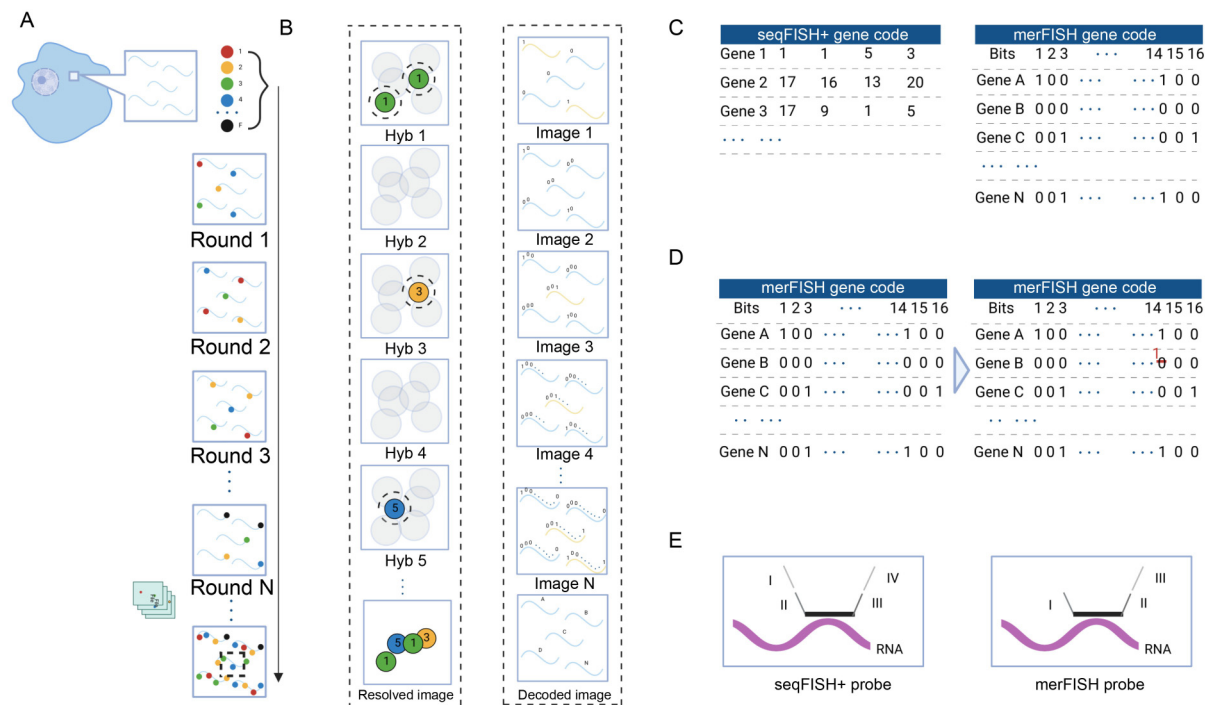


**Figure 2.** (A) A schematic flow chart of seqFISH+. (B) seqFISH+ pseudocolor is demonstrated on the left panel. The merFISH 4 out of 16 Hamming distance binary barcoding scheme is demonstrated on the right panel. (C) seqFISH+ decoding illustration. For example, if the resolved image is 1, 1, 5, 3, then the resolved image is identified as gene 1. (D) An illustration of merFISH error robust detection. (E) merFISH probe consists of six subunits: (i) a forward primer binding site, which is 20 nt in length, (ii) the first readout region (30 nt), (iii) targeting region (30 nt), (iv) the second readout region, which is also 30 nt in length, (v) the third readout region (20 nt), and (vi) a reverse primer binding site, which is 20 nt in length. The illustration of two probes shows I: the first 30-nt readout region; II: the second readout region (30 nt); III: the third readout region (30 nt). 30-nt targeting region is demonstrated between I and II..

## seqFISH+ imaging

When seqFISH imaging was conducted, expansion microscopy could be employed to enhance transcript density [3]. Amine could be added to the primary probe to interact with PAGE gel to lower the false positive by increasing the distance among primary probes. Expansion microscopy was not employed in seqFISH+ since pseudocolor was utilized in seqFISH+ to enhance robustness. The pseudocolors provided validity of images even when samples were enlarged due to water absorption.

## merFISH

Although smFISH [49,50] enables RNA quantification and localization, high-throughput FISH needs to be developed. Thus, with super-resolution imaging for smFISH and the strategy of combinatorial labeling [51], a binary barcode is generated for targeted sequence which could be referenced after imaging. Using this barcoding scheme, a new high-throughput FISH method was developed.

## Development of merFISH

merFISH was designed to conduct multiple smFISH simultaneously to achieve high-throughput scheme [20]. During each round of hybridization, smFISH's super-resolution imaging and combinatorial labeling would issue each RNA a binary code, "1" marks when fluorescent probe successfully hybridizes with targeted RNA; on the other hand, "0" marks when fluorescent probe did not hybridize with targeted RNA.

## Probe design for merFISH

Primary and secondary hybridization was employed in merFISH, primary probe consists of six subunits (Fig. 2E). The 30 nt targeting region is complementary to the RNA sequence; in addition, the first and second 30 nt flanking readout regions are used for probing, and both readout regions use the same code, 16-bits, same direction. The remaining two forward and reverse priming regions are used for probe extensions.

Three sections composed of a merFISH probe

(Fig. 2E), the central targeting sequence for *in situ* hybridization that is 50 nt long could hybridize with the targeted RNA sequence, and two flank readout sequences that locates on the both end of the central targeting sequence could readily bind with fluorescent probes. The flank readout sequence also effectively lowered the problem of background noise from failed probe hybridization.

### Error-robustness of merFISH

False detections are the biggest problem for high-throughput imaging. The reported false negative is 10%, and false positive is 4%. In order to lower misidentification rate contributed by background noise and contaminations from each round of probe should be washed off. merFISH applied Hamming distance (HD) to cross references marked RNA barcode with RNA probe library. In addition, hamming code can also perform error detection, when barcode is 1-bit off the RNA probe library, the correction will be activated to replace the error with corrected barcode, when barcode is 2-bits off the RNA probe library, the error will be notified. This approach could effectively enhance error-robustness.

By introducing HD code to the combinatorial labeling, an error-robustness scheme is employed for labeling and detecting errors. 140 RNA species were imaged in human fibroblast cells through 16-bits MHD4 (modified Hamming distance 4, where 16 bits barcodes separated with at least of HD4) code which is capable of both error detection and correction, and they imaged 1001 RNA species through MHD2 code which is capable of error detection but not correction [20].

merFISH employed 16-bits MHD4 code rather than 14-bits MHD2 since the prior has higher precision. The employment of 16-bits MHD4 code also contributed to differences for possible coding genes. 16-bits MHD4 marked 140 genes (130 genes and 10 misidentification control genes), each gene labeled with 198 primary probes. Two readout regions correspond with four readout sequences. For all 140 transcripts demonstrated in original merFISH paper [20], a total of 16 hybridization were used to generate 16 bits code for each transcript, and each bit were denoted with either “1” or “0”, determined by presence or absence of readout probe fluorescent. These 16 bits codes were further abided by Hamming distances 4, which means only four “1” were allowed in each 16 bits code.

### MerFISH protocol

The merFISH hybridization process on measuring the

specific copies of RNA demonstrated to be far more straight-forward compared with other fluorescent *in situ* hybridization methodologies, for example, merFISH procedure carries significantly more fluorescent probes compared to smFISH in order to comprehensively achieve RNAs multiplexing. In the merFISH experiment [52], the researchers utilized 150-nt as their primary probe to measure 140 RNA species. In the PCR, a 30-nt T7 promoter sequence was added. Due to the high demand of DNA oligonucleotides during the first hybridization (encoding probes, termed by the team), the incorporation of T7 promoter in transcription and reverse transcription satisfied high demanding probes.

In PCR, amplification was conducted along with the reverse primer and T7 promoter placed right next to it. The merFISH examined the optimal amplification condition through qPCR. 170  $\mu\text{L}$  (10  $\mu\text{L}$  used for quality examination, 160  $\mu\text{L}$  used for transcription) were obtained after purification while maintaining a 10–50 ng/ $\mu\text{L}$  concentration production.

In transcription, the Quick HiScribe T7 polymerase kit was employed in the merFISH experiment [52]. After 12 to 16 hours incubation (37 °C), 100  $\mu\text{L}$  of purified RNA (concentration ranging from 0.5–2 ng/ $\mu\text{L}$ ) were obtained. In Wu Lab merFISH protocol adapted from [20], T7 Oligopaint Synthesis output 7  $\mu\text{L}$  (from 1 $\times$  reaction: 20  $\mu\text{L}$ ; DNA oligonucleotide: 0.5–1  $\mu\text{g}$ ), which would require at least two additional PCR cycles to reach qualified concentration.

In reverse transcription, Wu lab protocol did not purify RNA, and Wu lab used 1 $\times$  reaction 150  $\mu\text{L}$  to conduct further reverse transcription (incubation at 50 °C for 2 hours and heated to 85 °C for 5 minutes and stopped reaction). On the other hand, Zhuang lab protocol utilized Maxima H- reverse transcriptase, and they added NaOH and EDTA in the termination reaction. Zhuang lab distributed the samples into 100  $\mu\text{g}$  ssDNA individual volumes and dried into powder form to mix with encoding probes for hybridizations.

In cellular treatment, the merFISH used 4% PFA for cross-linking and 0.5% v/v Triton X-100 for permeabilization buffer (placed in room temperature for 2 minutes). Encoding probe hybridization buffer and wash buffer contains 30% deionized formamide to optimize hybridization and wash off procedure. Vandyl Ribonucleoside Complex was added to inhibit RNase. Zhuang lab protocol recommended a 5–200  $\mu\text{M}$  encoding probe concentration for hybridization, a 12–36 hours incubation in 37 °C for optimized hybridization.

To expedite hybridization time between readout probe and encoding probe for maximum rounds of readout hybridization, Zhuang lab selected the 10 nM concentration readout probe to incubate at 37 °C for 15 minutes to complete hybridization. Compared to the

encoding probe, both the readout probe hybridization buffer (contained 10% deionized formamide) and wash off probe hybridization buffer (contained 20% deionized formamide) demonstrated to have less deionized formamide concentrations.

When imaging was completed, Zhuang lab protocol utilized the highest magnitude laser for quenching to ensure the next round of readout probing to be freshly hybridized. This is the most critical part of the procedure, once all the previous rounds of probes were quenched, the imaging of the next round could be successful.

## INTEGRATION OF DNA seqFISH+, RNA seqFISH AND IF

Although Hi-C [53] & SPRITE [54] could provide detailed data on chromosomal interactions in single cells, the spatial information of chromosome architectures are not yet to be demonstrated by bioimaging-based approaches. Thus, DNA seqFISH+ is coupled with RNA seqFISH and IF (immunofluorescence) to examine nuclear architecture at global level in single cells [26].

Since chromosomal structures demonstrated high variabilities across single cells, integration of DNA seqFISH+, RNA seqFISH, and IF [55] provided a seqFISH+ based spatial multi-omics approach, which was extended from the previous study [56]. In this method, a total of 3660 chromosomal loci were imaged using DNA seqFISH+, 17 chromatin markers and subnuclear structures were imaged using IF, and 70 RNA species were identified using RNA seqFISH, in mouse embryonic stem cells (mESC). In addition, through the integration of this new approach, the nuclei structure at 1 Mb resolution can be imaged comprehensively, and the 20 specific 1.5-Mb long regions can be imaged at 25 kb resolution [26]. This integration method started with RNA seqFISH hybridization, and then DNA seqFISH+ would be performed. Sequential IF hybridization was conducted at last.

### Integration of DNA seqFISH+, RNA seqFISH and IF to image the global-level genomic structure

The DNA seqFISH+ followed the seqFISH+ coding schematics, and 2460 loci were labeled from the first and second channel. 1267 loci at 2 Mb were targeted by the first channel at 643-nm, and 1193 loci at 5 primes ends were targeted by the second channel at 561 nm. Five rounds of DNA seqFISH+ barcoding was performed on a 16-based coding scheme, resulting in

4096 unique barcodes from the first three rounds of barcoding, and the remaining two rounds were used as parity check. In addition, the 16-pseudocolour base was obtained from hybridizing the 16 individual readout samples [26].

The third fluorescence channel targeted the remaining 1200 loci on 20 different chromosomes' 60 consecutive loci at 488 nm [26]. In the first 60 rounds of hybridization, 20 mouse chromosome (1200 chromosomal loci) would be readout one at a time. However, the distinction of each locus was unable to be identified and classified to each chromosome accordingly. Therefore, in the preceding 20 rounds of hybridization, the identification was revealed from probing the 1.5–2.4 Mb region individually and comprehensively. 1200 loci of the third channel could be decoded later. A total of 240 readouts (80 readouts per channel) were employed to fulfill this coding methodology.

### Probe design for the integrated imaging approach

Primary probes for DNA seqFISH+ are illustrated in Fig. 3. IF primary antibodies, conjugated with DNA oligonucleotides which could readily hybridize with fluorescence labels, were designed to target nuclear lamina [57], speckle [58], nucleolus [59], and chromatin markers [60]. RNA seqFISH probes were illustrated in Fig. 2E. Marker genes were selected based on previous mESCs studies [61–64].

This integrated DNA seqFISH+ approach reported a  $5616.5 \pm 1551.4$  dots per cell out of 446 cells with a false positive of only 0.25%, that is,  $14.0 \pm 7.4$  dots per cell [26]. The DNA seqFISH+ data demonstrated high agreement with Hi-C [65] and SPRITE [54] measurements.

Therefore, the integration of DNA seqFISH+, RNA seqFISH, and IF together provided a strategy that could be widely applied in the studies to image the global-level genomic structures (chromatin structures, nucleus lamina, epigenetic markers, and RNA transcriptions) at the same time in a single cell.

### DNA merFISH

Unlike merFISH, DNA merFISH provides a method to hybridize every TAD region located within the chromosome. DNA merFISH technique was initially introduced [66] to image the TADs regions on chr20, chr21, chr22, and chrX in IMR90 fibroblast cells. Four years later, DNA merFISH enhanced its robustness and enabled imaging of genome and transcriptome simultaneously by adding genome scale chromatin imaging based on the technique [55].

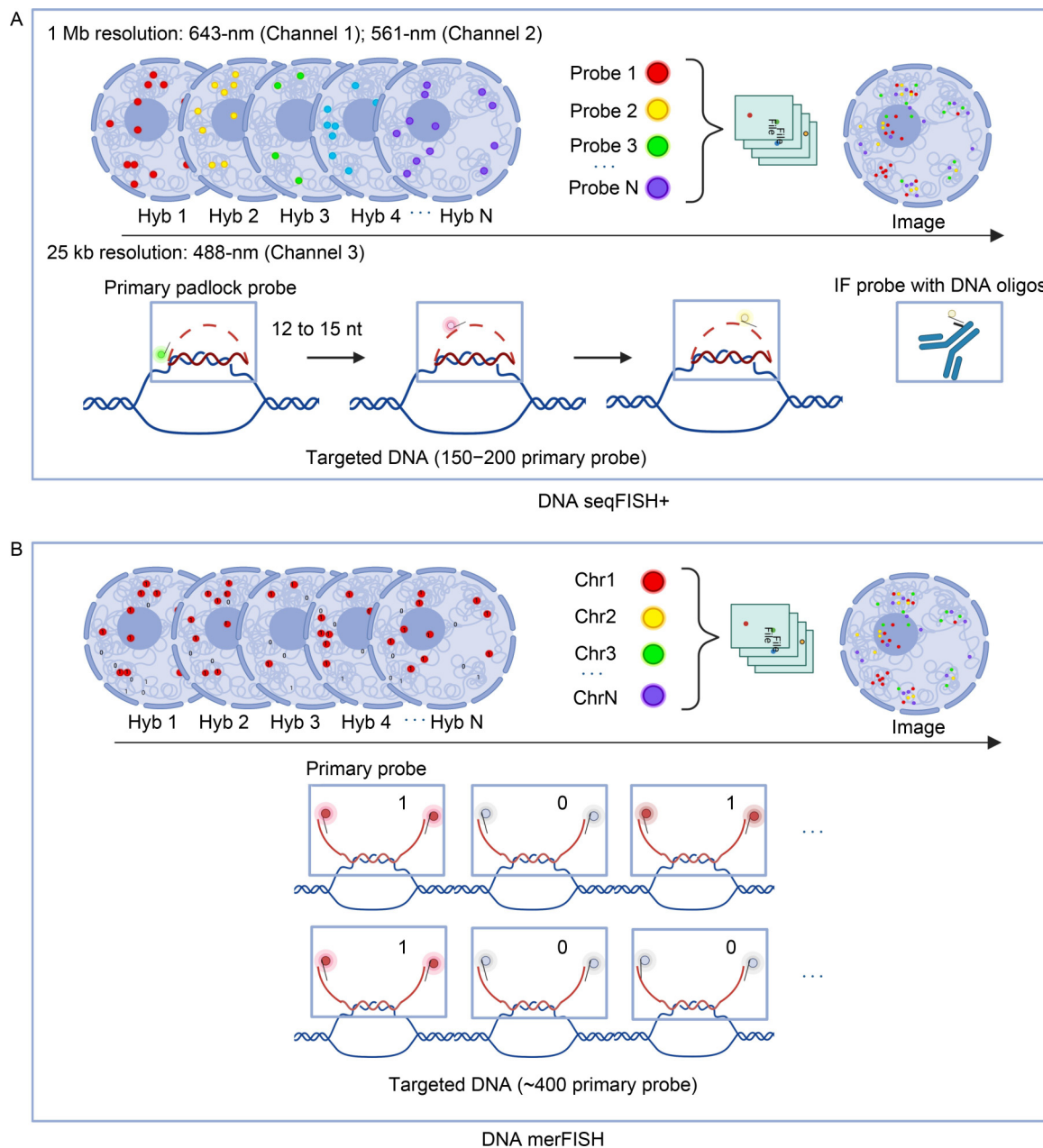


**Figure 3.** (A) A demonstration of integrated imaging approach using three channels to imaging a total of 3667 loci is shown here. DNA seqFISH+ probe: on Mb resolution, the primary probe consists a 35-nt sequence with five flanked unique 15 nt readout regions (demonstrate the corresponding signal to according pseudo-channel in each barcoding round), and primer binding sites (20 nt in length) at 5 prime and 3 prime end of the probe; on the kb resolution, the primary probe consists: 35-nt sequence with three flanked uniform readout probe that is 15 nt in length that correspond to the imaging diffraction limit, and two uniform binding sites for readout probe (15 nt in length), and primer binding sites (20 nt) of the probes that located at the 5 prime and 3 prime end (refer Fig. 2E). IF probes composed of antibody and DNA oligonucleotide are illustrated as well. (B) A multi-scale multiplexed FISH developed by Zhuang's lab along with the primary probe for genomic loci are demonstrated. Each primary probe contains a 30 nt readout sequence and a 40–42 nt target sequence complementary to the genomic loci..

### Whole-chromosome scale imaging

Whole-chromosome scale imaging, focused primarily on hybridizing the entire TADs regions within the

chromosome [66]. Through genomic sequence, based on TAD information obtained from Hi-C map, whole-chromosome scale imaging constructed its primary probe. Each TAD was targeted with 1000 primary

probes, and multiple rounds of hybridization would conduct until the entire TAD was hybridized. Once all the primary probes hybridize with all the targeted regions on DNA, the secondary probe with different colors of fluorophores would deploy to hybridize with the primary probes. Next, multiple rounds of hybridizations of these probes were repeated, until every targeted region could be identified throughout all the TADs.

As one application [66], a total of 34 TADs within chr21 of IMR90 fibroblast cell line were marked. Through 17 rounds of hybridizations, the 3D positions of the 34 TADs were confirmed. By removing all the unsuccessful hybridizations, a total of 120 chr21 from many cells were visualized, and the average spatial distance of these 34 TADs were obtained from measuring the spatial distances within the TAD area of these 120 chr21 [66]. The Pearson correlation coefficient between DNA merFISH and Hi-C results reached 0.91, suggesting DNA merFISH was well validated.

The same methodology applied in chr21 was also applied to 27 TADs from chr20 and 30 TADs from chr22. The imaging of these TADs showed promising results similar to that of chr21. In addition to marking all the TADs in chr20, 21, and 22, the researchers also marked 40 TADs within chromosome X through tracing

the position of the central 100-kb region of each of these 40 TADs. A total of 86 TADs' information were obtained from chrX. There are 86 TADs in total in chrX, from which 40 TADs were labeled and imaged.

## Genome-chromosome scale imaging

The development of DNA and hnRNA (heterogeneous RNA) hybridization

Hi-C and its derivative methods could not demonstrate the comprehensive spatial, especially geometric information for genomics data. As a result, a technique that could provide both DNA and RNA spatial information in a high-throughput manner is in need of development since chromatin interactions and the spatial organization of genomics plays important role for gene expressions in cells. Building on top of [66] method, both the spatial transcriptome and genome of Chr21. 650 50-kb segments were selected from Chr21 to function as the targeted region, and primary probes were constructed based on these targeted regions [55].

In order to label the most amount of the gene each round, the researchers used three fluorophores' probes, and each fluorophore is captured by one of the three channels (Table 2). As a result, a total of 650 segments on chr21 were labeled with three fluorophores in more than 200 rounds of hybridization in total. Genome-scale

**Table 2 The similarity and difference between RNA merFISH [20] and DNA merFISH [55,66]**

	Length of target region	Length of readout	Round	Number of readouts in one probe	Hamming weight	Result	Number of colors
merFISH [20]	30	20	16	2	4	140 gene in MHD4 & 1001 gene in MHD2	3'Cy5
2016 [66] Whole chr21	30	30	17	1		34 TADs	5'Alexa Fluor 647 and ATTO 565 modifications
Whole chr22	30	30	14 probes labeled with Alex647 and 13 probes labeled with ATTO565	1		27 TADs	5'Alexa Fluor 647 and ATTO 565 modifications
Whole chr20	30	30	15	1		30 of the 60 TADs	5'Alexa Fluor 647 and ATTO 565 modifications
Whole chrX	30	30	20	1		40 TADs (out of 86 total)	5'Alexa Fluor 647 and ATTO 565 modifications
2020 [55] Whole chr21	42	20	More than 200 in three channels	3		651 target genomic loci	5' Alexa750, Alexa647 or Cy5, and Cy3
Whole chr21 (nascent RNA)	30	20		4		~80 genes interspersed across chr21	Cy3, Cy5 (or Alexa647) and Alexa750
Whole chr2	42	20	More than 300 in three channels	2		4844 target genomic loci	5' Cy3, Cy5 and Alexa750
Genome-scale	40	20	50 rounds of hybridization and 2 color channels per round	2	2	1041 genomic loci	5' & 3' Cy5 and Alexa750
Genome-scale (nascent RNA)	40	20	18 rounds in 3 colors	3	2	1137 genes	5' Cy3, Cy5 and Alexa750

chromatin imaging was then applied to chr21 after whole-chromosome scale imaging to prevent DNA denaturing (RNA would be imaged prior to DNA in DNA merFISH. RNA intron probes would be hybridized for multiple rounds first. Then, the RNA introns probes would be washed off by RNase A to prepare the latter DNA imaging).

Genome-scale chromatin imaging innovatively utilized binary barcode Hamming weight of 2 (HW2), where each barcode contains two “1” s and 98 “0” s encompassing a total of 100-bits which correspond to 100 readout sequences, to demonstrate the highlight of DNA merFISH. Primary probes and secondary probes were designed the same way as merFISH. The 100 readout sequences were bound with Alex750 and Cy5 fluorophore individually. With two fluorescent probes being added in each hybridization round, 1000 genomic loci’s spatial information could be obtained through 50 rounds of hybridization.

In genome-scale chromatin imaging application, a total of 1041 genomic loci’s spatial locations ranging from 22 pairs of chromosomes along with X-chromosomes were constructed with 30 to 80 genomic loci targeted in each chromosome. Both whole-chromosome scale and genome-scale chromatin imaging were dedicated to label both chromosomal DNA and transcriptome/pre-RNAs simultaneously. The image of 1041 genomic locus and 1137 pre-RNAs were obtained in this work [55].

For whole-chromosome imaging, the researchers segmented the chromosomal DNA into 50 kb fragments, the target region was selected by removing the duplicates. The researchers selected 651 genomic loci on chr21 and 4844 genomic loci on chr2 as targeted region. The target sequence of probe is designed to hybridize every 50 kb fragments, where every 50 kb fragment should hybridize with 500 generated probes. Amongst the 500 probes generated, only the middle 250 to 360 were selected for labeling. All 651 targeted segments from chr21 were imaged successfully. One fifth of 4844, ~970, targeted segments from chr2 were imaged successfully since a 250 kb genomic resolution was required.

For the nascent RNA of chr21, the researchers selected 80 genes to construct primary probes that could label across 50 genomic loci. Primary probe’s target region was developed based on RNA intron to ensure the primary probe would hybridize with nuclear RNA precursors. The researchers also selected 5-kb up and downstream of TSS (transcription start site) to identify the initiation point of transcription.

In genome-scale chromatin imaging, the researchers selected 1041 genomic loci on 22 autosome and chrX in IMR90 fibroblast cell for imaging. Each chromosome

contains around 30 to 80 genomic loci that is around 30 kb in size. 1137 nascent RNA, located at these loci as well, were imaged at the same time using three color multiple rounds merFISH strategy.

## **MINA**

In order to image DNA, RNA at the same time at large scale, MINA (multiplexed imaging of nucleome architectures), a combination of the techniques of chromatin tracing and RNA merFISH [25], was developed to demonstrate mouse hepatocytes nucleome organization and expression. A schematic demonstration of MINA is demonstrated in Fig. 4.

### **Development of the MINA method**

MINA was used to label 50 central 100 kb TADs on chr19 and 195 kb segments upstream of the gene *Scd2*, which is stearyl-CoA desaturase 2 [25]. In chromatin tracing, each primary oligonucleotide probe consists of a designed genomic sequence to hybridize the targeted region and a non-genomic region with the same genomic sequence, which are designed to hybridize dye-labeled secondary probes. The secondary probes consist of a complementary sequence of the non-genomic sequence shared by all primary oligonucleotide probes. The spatial organizations were visualized.

A total of 69 secondary probes were utilized to denote 69 probed genomic regions [25]. In RNA merFISH, each primary oligonucleotide probe contains the targeting sequences which is complementary to designated RNA sequences and a 4 out of 16 readout sequence (MHD4) that could ascribe each RNA with a unique barcode. 55 major marker genes were found to be expressed into fetal liver cells from the 137 RNA species that were probed, and the remaining 82 were genes from chr19 [25]. Immunofluorescence staining of fibrillarlin was used to label nucleoli, and SYTOX or DAPI stain was used to image the whole nuclei [25].

### **RNA merFISH probe design**

A unique barcode was assigned to each RNA species using MHD4 as discussed in the merFISH section. The transcript sequences of 55 major marker genes and 82 genes located on chr19 were used to design the targeting regions. Probe design for chromatin tracing and MINA imaging are discussed in Fig. 4.

### **Validation of MINA measurement**

MINA measurements were cross validated with established sequencing data. A total of 1225 pairwise distances obtained from each pair of TADs’s mean

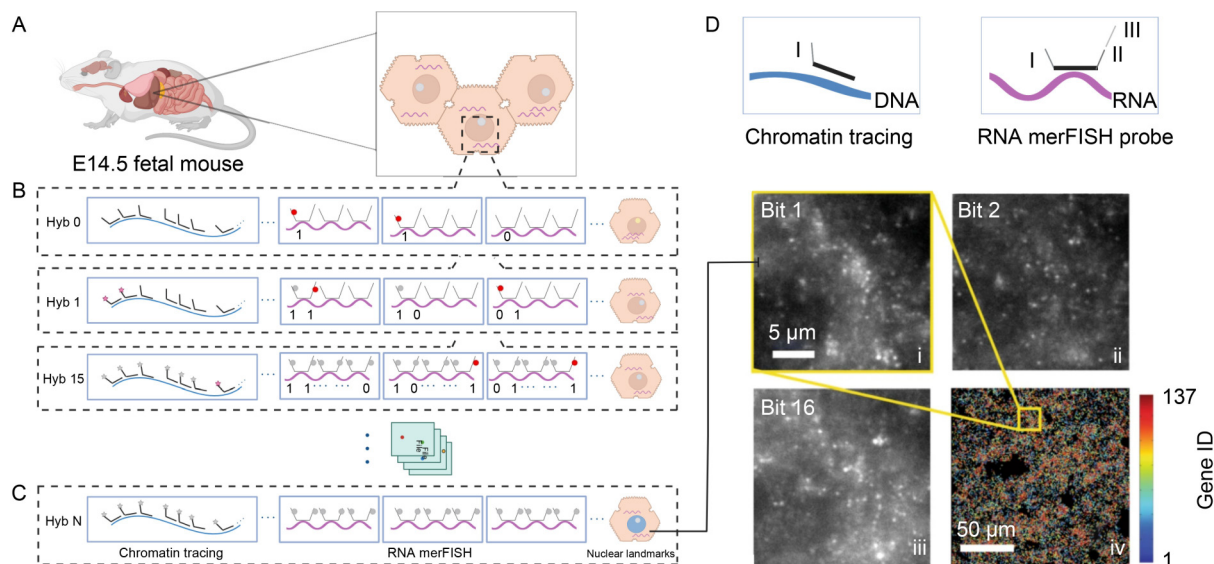


**Figure 4.** (A) The schematic illustration of MINA and its subject and imaging location. MINA was first applied on the subject E14.5 fetal mouse liver cell. (B) ATTO 565 and Alexa Fluor 647 corresponding secondary probes (30 nt) were employed for tracing chromatin; for RNA merFISH, Alexa Fluor 750 paired secondary probes (20 nt) were employed. Both secondary probes were complementary to their readout regions. A total of 40 rounds of secondary hybridizations were performed, 750-nm channel was used to image from pre-hyb (hyb 0) to hyb 15, 647 nm channel was used to image the first 40 TADs on chr19 (hyb 1 to hyb 40), 560 nm channel was used to image the last 10 TADs on chr19 (hyb 21 to hyb 30), and 560 nm channel was used again to image the 19 consecutive loci upstream of *scd2* (hyb 1 to hyb 19). (C) Image of RNA molecules after secondary hybridization. All identified RNA molecules are referenced to their gene ID on the right. The yellow box on (iv) is the uniform region of i – iii. The picture is extracted from [25]. (D) Chromatin tracing probe: the template probe for tracing of 50 TADs of fetal mouse chr19 consisted of four regions (from 5 prime to 3 prime): (i) a forward primer binding site (20 nt in length), (ii) readout region (30 nt in length), (iii) a targeting region (30 nt in length), and (iv) a reverse primer binding site (20 nt in length). The genomic sequences of the central 100-kb of each TAD were used to construct the targeting regions. The illustration demonstrated the readout and targeting region (both 30 nt in length). RNA merFISH probe: each RNA merFISH template contains six regions (from 5 prime to 3 prime): (i) forward primer binding site, which is 20nt in length, (ii) a readout region (20 nt), (iii) a targeting region (30 nt), (iv) a second readout region (20 nt), (v) a third readout region (20 nt), followed by (vi) a reverse primer binding site, which is 20 nt in length..

spatial distance were compared with corresponding TADs data obtained using Hi-C contact frequencies. As a result, the mean spatial distances were found to be inversely correlated with Hi-C contact frequencies [25]. The merFISH results obtained using MINA were also compared with the bulk RNA sequencing data [25]. MINA demonstrated its robustness through these validations.

### MINA future application

As a systemic, high throughput spatially imaging approach to obtain the measurements of diverse RNA species' copy number, chromatin folding, and the association of various genomic regions with nucleoli, nuclear lamina, and surface of chromosomes in single cells, MINA offered a multiplexed imaging way to observe across various mammalian tissue's chromatin and nucleosome structures on the single cells level.

MINA also demonstrated capability of mapping cell-type-specific chromatin structure to evaluate its expression. MINA is expected to be widely applied to map other many, not only mammalian tissue's nucleosome architectures [25].

### CHALLENGES AND PERSPECTIVE

Over the past decades, the development of FISH has been fueled with innovations, from ISH to multiplexed and high-throughput methodologies. For example, OligoFISSEQ [67] provides a comprehensive view of the transcriptome due to the high spatial resolution and high-throughput sequencing, by enabling the simultaneous detection and sequencing of multiple RNAs within a single cell or tissue specimen.

For further development of bioimaging-based spatial multi-omic methodologies, enhancing imaging resolutions shall be one of the most fundamental challenges.

Minflux [68] and other advanced super-resolution microscopy with higher spatial resolution can be used for resolution enhancement.

Time expenditure is another fundamental challenge. Automatization of multiple rounds of hybridization is a must to reduce in labor and to save the time for multiplex FISH. More automatization instruments will be developed to offer solution with higher sensitivity in a timely manner.

The third challenge is the imaging accuracy. FISH signals should be identified from noisy background precisely. The errors could be contributed by the samples or equipment in the form of inaccurate measurements [69,70]. Through machine learning based artificial intelligence methods, the signal to noise ratio could be further improved and the accuracy of FISH would increase significantly.

With significant improvement mentioned above, bioimaging-based spatial multi-omic methodologies will be able to play more important roles in the future.

## CONCLUSION

In this review, several image-based multi-omic methods, including, seqFISH, seqFISH+, merFISH, integration DNA seqFISH+, DNA merFISH, and MINA, are introduced here, along with their probe design and imaging procedures. SeqFISH+ incorporated 60 pseudocolors to enhance imaging capability and enable more images per channel. merFISH utilized modified Hamming weight of 4 to introduce error-detection ability to FISH. DNA seqFISH+ can be integrated with RNA seqFISH and IF to image nuclear architecture on a global scale in single cells. DNA merFISH enables imaging of transcriptome and genome at the same time. MINA introduced comprehensive imaging of nucleome in a high throughput manner on mammalian tissues.

If we compare merFISH, visium from 10× Genomics, and other methods, we will find that, (i) merFISH demonstrated impressive resolution on imaging and error-detection capability, whereas 10× Genomics shown robustness ability on finding unidentified transcripts by using poly-T as adaptors on flow cell. (ii) Though the method to visualize multiple genomic loci through multiple rounds of DNA hybridizations not only relied heavily on primary probe design but also demonstrated limitations on the amount of subject to be studied each time since one conduction of multiple rounds of DNA hybridizations could only generate data for one chromosome, but this kind of method remains a power tool when demonstrating TAD structure and transcription data in the single cell. In conclusion, a high throughput *in situ* fluorescent hybridization method that could be used to identify cell types and development is

profound and impactful. In general, this review provides a survey of these spatial-multi-omics techniques in hopes of benefiting researchers on selecting appropriate technique for their research.

## COMPLIANCE WITH ETHICS GUIDELINES

**Conflicts of interest** The authors Yan Yan, Liheng Yang, Leyuan Meng, Haochen Su, Cheng Zhou, Le Yu, Zhengtu Li, Xu Zhang, Huihua Cai and Juntao Gao declare that they have no competing interests.

The article is a review and does not contain any human or animal subjects performed by any of the authors.

## OPEN ACCESS

This article is licensed by the CC BY under a Creative Commons Attribution 4.0 International License, which permits use, sharing, adaptation, distribution and reproduction in any medium or format, as long as you give appropriate credit to the original author(s) and the source, provide a link to the Creative Commons licence, and indicate if changes were made. The images or other third party material in this article are included in the article's Creative Commons licence, unless indicated otherwise in a credit line to the material. If material is not included in the article's Creative Commons licence and your intended use is not permitted by statutory regulation or exceeds the permitted use, you will need to obtain permission directly from the copyright holder. To view a copy of this licence, visit <http://creativecommons.org/licenses/by/4.0/>.

## REFERENCES

- Andersson, R., Gebhard, C., Miguel-Escalada, I., Hoof, I., Bornholdt, J., Boyd, M., Chen, Y., Zhao, X., Schmidl, C., Suzuki, T., *et al.* (2014) An atlas of active enhancers across human cell types and tissues. *Nature*, 507, 455–461
- Bintu, B., Mateo, L. J., Su, J.-H., Sinnott-Armstrong, N. A., Parker, M., Kinrot, S., Yamaya, K., Boettiger, A. N., and Zhuang, X. (2018) Super-resolution chromatin tracing reveals domains and cooperative interactions in single cells. *Science*. 362, eaau1783
- Shah, S., Lubeck, E., Zhou, W. and Cai, L. (2016) *In situ* transcription profiling of single cells reveals spatial organization of cells in the mouse hippocampus. *Neuron*, 92, 342–357
- Wang, X., Allen, W. E., Wright, M. A., Sylwestrak, E. L., Samusik, N., Vesuna, S., Evans, K., Liu, C., Ramakrishnan, C., Liu, J., *et al.* (2018) Three-dimensional intact-tissue sequencing of single-cell transcriptional states. *Science*, 361, eaat5691
- Guan, M., Wang, M., Zhanghao, K., Zhang, X., Li, M., Liu, W., Niu, J., Yang, X., Chen, L., Jing, Z., *et al.* (2022) Polarization modulation with optical lock-in detection reveals universal fluorescence anisotropy of subcellular structures in live cells. *Light Sci. Appl.*, 11, 4
- Chen, L., Wang, M., Zhang, X., Zhang, M., Hu, Y., Shi, Z., Xi, P. and Gao, J. (2019) Group-sparsity-based super-resolution dipole orientation mapping. *IEEE Trans. Med. Imaging*, 38, 2687–2694

7. Yang, X., Zhanghao, K., Wang, H., Liu, Y., Wang, F., Zhang, X., Shi, K., Gao, J., Jin, D. and Xi, P. (2016) Versatile application of fluorescent quantum dot labels in super-resolution fluorescence microscopy. *ACS Photonics*, 3, 1611–1618
8. Zhanghao, K., Chen, L., Yang, X.-S., Wang, M.-Y., Jing, Z.-L., Han, H.-B., Zhang, M. Q., Jin, D., Gao, J.-T. and Xi, P. (2016) Super-resolution dipole orientation mapping via polarization demodulation. *Light Sci. Appl.*, 5, e16166
9. Kishi, J. Y., Lapan, S. W., Beliveau, B. J., West, E. R., Zhu, A., Sasaki, H. M., Saka, S. K., Wang, Y., Cepko, C. L. and Yin, P. (2019) SABER amplifies FISH: enhanced multiplexed imaging of RNA and DNA in cells and tissues. *Nat. Methods*, 16, 533–544
10. Mota, A., Berezicki, S., Wernersson, E., Harbers, L., Li-Wang, X., Gradin, K., Peuckert, C., Crosetto, N. and Bienko, M. (2022) FRET-FISH probes chromatin compaction at individual genomic loci in single cells. *Nat. Commun.*, 13, 6680
11. Lyu, X.-Y., Deng, Y., Huang, X.-Y., Li, Z.-Z., Fang, G.-Q., Yang, D., Wang, F.-L., Kang, W., Shen, E.-Z. and Song, C.-Q. (2022) CRISPR FISHer enables high-sensitivity imaging of nonrepetitive DNA in living cells through phase separation-mediated signal amplification. *Cell Res.*, 32, 969–981
12. Banet, G., Bibi, O., Matouk, I., Ayesh, S., Laster, M., Kimber, K. M., Tykocinski, M., de Groot, N., Hochberg, A. and Ohana, P. (2000) Characterization of human and mouse H19 regulatory sequences. *Mol. Biol. Rep.*, 27, 157–165
13. Catena, R., Tiveron, C., Ronchi, A., Porta, S., Ferri, A., Tatangelo, L., Cavallaro, M., Favaro, R., Ottolenghi, S., Reinbold, R., *et al.* (2004) Conserved POU binding DNA sites in the Sox2 upstream enhancer regulate gene expression in embryonic and neural stem cells. *J. Biol. Chem.*, 279, 41846–41857
14. Krebsbach, P. H., Nakata, K., Bernier, S. M., Hatano, O., Miyashita, T., Rhodes, C. S. and Yamada, Y. (1996) Identification of a minimum enhancer sequence for the type II collagen gene reveals several core sequence motifs in common with the link protein gene. *J. Biol. Chem.*, 271, 4298–4303
15. Chi, X., Chatterjee, P. K., Wilson, W. 3rd, Zhang, S.-X., Demayo, F. J. and Schwartz, R. J. (2005) Complex cardiac Nkx2-5 gene expression activated by noggin-sensitive enhancers followed by chamber-specific modules. *Proc. Natl. Acad. Sci. USA*, 102, 13490–13495
16. Danielian, P. S., Echelard, Y., Vassileva, G. and McMahon, A. P. (1997) A 5.5-kb enhancer is both necessary and sufficient for regulation of Wnt-1 transcription *in vivo*. *Dev. Biol.*, 192, 300–309
17. Strachan, T. and Read, A. P. (2011). *Human Molecular Genetics*. New York: Garland Science/Taylor & Francis Group
18. Lubeck, E., Coskun, A. F., Zhiyentayev, T., Ahmad, M. and Cai, L. (2014) Single-cell *in situ* RNA profiling by sequential hybridization. *Nat. Methods*, 11, 360–361
19. Eng, C. L., Lawson, M., Zhu, Q., Dries, R., Koulena, N., Takei, Y., Yun, J., Cronin, C., Karp, C., Yuan, G.-C., *et al.* (2019) Transcriptome-scale super-resolved imaging in tissues by RNA seqFISH. *Nature*, 568, 235–239
20. Chen, K. H., Boettiger, A. N., Moffitt, J. R., Wang, S. and Zhuang, X. (2015) RNA imaging. Spatially resolved, highly multiplexed RNA profiling in single cells. *Science*, 348, aaa6090d
21. Moffitt, J. R., Hao, J., Bambah-Mukku, D., Lu, T., Dulac, C. and Zhuang, X. (2016) High-performance multiplexed fluorescence *in situ* hybridization in culture and tissue with matrix imprinting and clearing. *Proc. Natl. Acad. Sci. USA*, 113, 14456–14461
22. Liu, M., Yang, B., Hu, M., Radda, J. S. D., Chen, Y., Jin, S., Cheng, Y. and Wang, S. (2021) Chromatin tracing and multiplexed imaging of nucleome architectures (MINA) and RNAs in single mammalian cells and tissue. *Nat. Protoc.*, 16, 2667–2697
23. Niu, J., Zhang, X., Li, G., Yan, P., Yan, Q., Dai, Q., Jin, D., Shen, X., Wang, J., Zhang, M. Q., *et al.* (2020) A novel cytogenetic method to image chromatin interactions at subkilobase resolution: Tn5 transposase-based fluorescence *in situ* hybridization. *J. Genet. Genomics*, 47, 727–735
24. Jia, B. B., Jussila, A., Kern, C., Zhu, Q. and Ren, B. (2023) A spatial genome aligner for resolving chromatin architectures from multiplexed DNA fish. *Nat. Biotechnol.*, 41, 1004–1017
25. Liu, M., Lu, Y., Yang, B., Chen, Y., Radda, J. S. D., Hu, M., Katz, S. G. and Wang, S. (2020) Multiplexed imaging of nucleome architectures in single cells of mammalian tissue. *Nat. Commun.*, 11, 2907
26. Takei, Y., Yun, J., Zheng, S., Ollikainen, N., Pierson, N., White, J., Shah, S., Thomassie, J., Suo, S., Eng, C. L., *et al.* (2021) Integrated spatial genomics reveals global architecture of single nuclei. *Nature*, 590, 344–350
27. Ni, Y., Cao, B., Ma, T., Niu, G., Huo, Y., Huang, J., Chen, D., Liu, Y., Yu, B., Zhang, M. Q., *et al.* (2017) Super-resolution imaging of a 2.5 kb non-repetitive DNA *in situ* in the nuclear genome using molecular beacon probes. *eLife*, 6, e21660
28. Xie, S. Q., Lavitas, L.-M., and Pombo, A. (2010) Cryofish: fluorescence *in situ* hybridization on ultrathin cryosections. *Methods Mol. Biol.*, 659, 219–230
29. Bienko, M., Crosetto, N., Teytelman, L., Klemm, S., Itzkovitz, S., and Van Oudenaarden, A. (2013) A versatile genome-scale PCR-based pipeline for high-definition DNA FISH. *Nat. Methods*, 10, 122–124
30. Beliveau, B. J., Joyce, E. F., Apostolopoulos, N., Yilmaz, F., Fonseka, C. Y., McCole, R. B., Chang, Y., Li, J. B., Senaratne, T. N., Williams, B. R., *et al.* (2012) Versatile design and synthesis platform for visualizing genomes with oligopaint FISH probes. *Proc. Natl. Acad. Sci. USA*, 109, 21301–21306
31. Beliveau, B. J., Boettiger, A. N., Avendaño, M. S., Jungmann, R., McCole, R. B., Joyce, E. F., Kim-Kiselak, C., Bantignies, F., Fonseka, C. Y., Erceg, J., *et al.* (2015) Single-molecule super-resolution imaging of chromosomes and *in situ* haplotype visualization using oligopaint FISH probes. *Nat. Commun.*, 6, 7147
32. Deng, W., Shi, X., Tjian, R., Lionnet, T. and Singer, R. H. (2015) CASFISH: CRISPR/Cas9-mediated *in situ* labeling of genomic

- loci in fixed cells. *Proc. Natl. Acad. Sci. USA*, 112, 11870–11875
33. Wang, H., Nakamura, M., Abbott, T. R., Zhao, D., Luo, K., Yu, C., Nguyen, C. M., Lo, A., Daley, T. P., La Russa, M., *et al.* (2019) CRISPR-mediated live imaging of genome editing and transcription. *Science*, 365, 1301–1305
  34. Mateo, L. J., Murphy, S. E., Hafner, A., Cinquini, I. S., Walker, C. A. and Boettiger, A. N. (2019) Visualizing DNA folding and RNA in embryos at single-cell resolution. *Nature*, 568, 49–54
  35. Dandachi, N., Dietze, O. and Hauser-Kronberger, C. (2002) Chromogenic *in situ* hybridization: a novel approach to a practical and sensitive method for the detection of HER2 oncogene in archival human breast carcinoma. *Lab. Invest.*, 82, 1007–1014
  36. Cuadrado, A., Golczyk, H. and Jouve, N. (2009) A novel, simple and rapid nondenaturing FISH (ND-FISH) technique for the detection of plant telomeres. Potential used and possible target structures detected. *Chromosome Res.*, 17, 755–762
  37. Sekar, R., Pernthaler, A., Pernthaler, J., Warnecke, F., Posch, T. and Amann, R. (2003) An improved protocol for quantification of freshwater Actinobacteria by fluorescence *in situ* hybridization. *Appl. Environ. Microbiol.*, 69, 2928–2935
  38. van Krieken, J. H. (2009) New developments in the pathology of malignant lymphoma: a review of the literature published from August to November 2009. *J. Hematop.*, 2, 245–251
  39. Bayani, J., and Squire, J. A. (2004) Fluorescence *in situ* hybridization (FISH). *Curr. Protoc. Cell Biol.*, 23, 22.24. 21–22.24. 52
  40. Kallioniemi, A., Kallioniemi, O.-P., Sudar, D., Rutovitz, D., Gray, J. W., Waldman, F. and Pinkel, D. (1992) Comparative genomic hybridization for molecular cytogenetic analysis of solid tumors. *Science*, 258, 818–821
  41. Jackson, S. A., Wang, M. L., Goodman, H. M. and Jiang, J. (1998) Application of fiber-FISH in physical mapping of *Arabidopsis thaliana*. *Genome*, 41, 566–572
  42. Rufer, N., Dragowska, W., Thornbury, G., Roosnek, E. and Lansdorp, P. M. (1998) Telomere length dynamics in human lymphocyte subpopulations measured by flow cytometry. *Nat. Biotechnol.*, 16, 743–747
  43. Chen, C., Hong, Y.-K., Ontiveros, S. D., Egholm, M. and Strauss, W. M. (1999) Single base discrimination of CENP-B repeats on mouse and human chromosomes with PNA-FISH. *Mamm. Genome*, 10, 13–18
  44. Koch, J. E., Kølvrå, S., Petersen, K. B., Gregersen, N. and Bolund, L. (1989) Oligonucleotide-priming methods for the chromosome-specific labelling of alpha satellite DNA *in situ*. *Chromosoma*, 98, 259–265
  45. Schwarzacher, T., Leitch, A., Bennett, M. D. and Heslop-Harrison, J. (1989) *In situ* localization of parental genomes in a wide hybrid. *Ann. Bot. (Lond.)*, 64, 315–324
  46. Yamamoto, M. and Mukai, Y. (1989) Application of fluorescence *in situ* hybridization to molecular cytogenetics of wheat. *Wheat Inf. Serv.*, 69, 30–32
  47. Pardue, M. L. and Gall, J. G. (1969) Molecular hybridization of radioactive DNA to the DNA of cytological preparations. *Proc. Natl. Acad. Sci. USA*, 64, 600–604
  48. John, H. A., Birnstiel, M. L. and Jones, K. W. (1969) RNA-DNA hybrids at the cytological level. *Nature*, 223, 582–587
  49. Femino, A. M., Fay, F. S., Fogarty, K. and Singer, R. H. (1998) Visualization of single RNA transcripts *in situ*. *Science*, 280, 585–590
  50. Raj, A., van den Bogaard, P., Rifkin, S. A., van Oudenaarden, A. and Tyagi, S. (2008) Imaging individual mRNA molecules using multiple singly labeled probes. *Nat. Methods*, 5, 877–879
  51. Lubeck, E. and Cai, L. (2012) Single-cell systems biology by super-resolution imaging and combinatorial labeling. *Nat. Methods*, 9, 743–748
  52. Moffitt, J. R. and Zhuang, X. (2016) Rna imaging with multiplexed error-robust fluorescence *in situ* hybridization (merFISH). *Methods Enzymol.*, 1–49
  53. Lieberman-Aiden, E., van Berkum, N. L., Williams, L., Imakaev, M., Ragozy, T., Telling, A., Amit, I., Lajoie, B. R., Sabo, P. J., Dorschner, M. O., *et al.* (2009) Comprehensive mapping of long-range interactions reveals folding principles of the human genome. *Science*, 326, 289–293
  54. Quinodoz, S. A., Ollikainen, N., Tabak, B., Palla, A., Schmidt, J. M., Detmar, E., Lai, M. M., Shishkin, A. A., Bhat, P., Takei, Y., *et al.* (2018) Higher-order inter-chromosomal hubs shape 3D genome organization in the nucleus. *Cell*, 174, 744–757.e24
  55. Su, J.-H., Zheng, P., Kinrot, S. S., Bintu, B., and Zhuang, X. (2020) Genome-scale imaging of the 3D organization and transcriptional activity of chromatin. *Cell*. 182, 1641–1659.e1626
  56. Takei, Y., Shah, S., Harvey, S., Qi, L. S. and Cai, L. (2017) Multiplexed dynamic imaging of genomic loci by combined CRISPR imaging and DNA sequential FISH. *Biophys. J.*, 112, 1773–1776
  57. van Steensel, B. and Belmont, A. S. (2017) Lamina-associated domains: links with chromosome architecture, heterochromatin, and gene repression. *Cell*, 169, 780–791
  58. Lamond, A. I. and Spector, D. L. (2003) Nuclear speckles: a model for nuclear organelles. *Nat. Rev. Mol. Cell Biol.*, 4, 605–612
  59. Pederson, T. (2011) The nucleus introduced. *Cold Spring Harb. Perspect. Biol.*, 3, a000521
  60. Ludwig, C. H. and Bintu, L. (2019) Mapping chromatin modifications at the single cell level. *Development*, 146, dev170217
  61. Shah, S., Takei, Y., Zhou, W., Lubeck, E., Yun, J., Eng, C. L., Koulou, N., Cronin, C., Karp, C., Liaw, E. J., *et al.* (2018) Dynamics and spatial genomics of the nascent transcriptome by intron seqfish. *Cell*, 174, 363–376.e16
  62. Singer, Z. S., Yong, J., Tischler, J., Hackett, J. A., Altinok, A., Surani, M. A., Cai, L. and Elowitz, M. B. (2014) Dynamic heterogeneity and DNA methylation in embryonic stem cells. *Mol. Cell*, 55, 319–331
  63. Kolodziejczyk, A. A., Kim, J. K., Tsang, J. C., Ilicic, T., Henriksson, J., Natarajan, K. N., Tuck, A. C., Gao, X., Bühler, M., Liu, P., *et al.* (2015) Single cell RNA-sequencing of

- pluripotent states unlocks modular transcriptional variation. *Cell Stem Cell*, 17, 471–485
64. Hormoz, S., Singer, Z. S., Linton, J. M., Antebi, Y. E., Shraiman, B. I. and Elowitz, M. B. (2016) Inferring cell-state transition dynamics from lineage trees and endpoint single-cell measurements. *Cell Syst.*, 3, 419–433.e8
65. Bonev, B., Mendelson Cohen, N., Szabo, Q., Fritsch, L., Papadopoulos, G. L., Lubling, Y., Xu, X., Lv, X., Hugnot, J.-P., Tanay, A., *et al.* (2017) Multiscale 3D genome rewiring during mouse neural development. *Cell*, 171, 557–572.e24
66. Wang, S., Su, J.-H., Beliveau, B. J., Bintu, B., Moffitt, J. R., Wu, C. T. and Zhuang, X. (2016) Spatial organization of chromatin domains and compartments in single chromosomes. *Science*, 353, 598–602
67. Nguyen, H. Q., Chatteraj, S., Castillo, D., Nguyen, S. C., Nir, G., Lioutas, A., Hershberg, E. A., Martins, N. M. C., Reginato, P. L., Hannan, M., *et al.* (2020) 3D mapping and accelerated super-resolution imaging of the human genome using *in situ* sequencing. *Nat. Methods*, 17, 822–832
68. Schmidt, R., Weihs, T., Wurm, C. A., Jansen, I., Rehman, J., Sahl, S. J. and Hell, S. W. (2021) MINFLUX nanometer-scale 3D imaging and microsecond-range tracking on a common fluorescence microscope. *Nat. Commun.*, 12, 1478
69. Wolf, D. E., Samarasekera, C. and Swedlow, J. R. (2007) Quantitative analysis of digital microscope images. *Methods Cell Biol.*, 81, 365–396
70. Joglekar, A. P., Salmon, E. D. and Bloom, K. S. (2008) Counting kinetochore protein numbers in budding yeast using genetically encoded fluorescent proteins. *Methods Cell Biol.*, 85, 127–151